Osma-Pinto, German; Ordóñez-Plata, Gabriel

Article

Measuring the effect of forced irrigation on the front surface of PV panels for warm tropical conditions

Energy Reports

Provided in Cooperation with:
Elsevier

Suggested Citation: Osma-Pinto, German; Ordóñez-Plata, Gabriel (2019) : Measuring the effect of forced irrigation on the front surface of PV panels for warm tropical conditions, Energy Reports, ISSN 2352-4847, Elsevier, Amsterdam, Vol. 5, pp. 501-514, https://doi.org/10.1016/j.egyr.2019.04.010

Energy Reports 5 (2019) 501–514

Contents lists available at ScienceDirect

Energy Reports

journal homepage: www.elsevier.com/locate/egyr

Research paper

Measuring the effect of forced irrigation on the front surface of PV panels for warm tropical conditions

German Osma-Pinto *, Gabriel Ordóñez-Plata

Universidad Industrial de Santander, Bucaramanga, 680002, Colombia

HIGHLIGHTS

- An irrigated PV panel can experiment direct and indirect cooling, and heating.
- Irrigating is attractive only for values of solar irradiation greater than 500 W/m^2.
- Irrigating can increase up to 10% of the daily energy generation of a PV panel.
- Energy benefit by irrigation depends strongly on irrigation time and power of pump.
- Discontinuous irrigation cycles can be more viable than continuous irrigation.

ARTICLE INFO

Article history:
Received 26 October 2018
Received in revised form 20 March 2019
Accepted 23 April 2019
Available online xxxx

Keywords:
PV generation
Cooling method
Irrigation
Energy efficiency

ABSTRACT

Irrigating the front surface of a PV panel is one method for reducing its operating temperature, thus increasing the output power. Several studies have investigated this method. Nevertheless, information on the thermal effects and energy benefits provided by irrigation over several operating cycles and water flow rates in warm-tropical conditions is lacking. Thus, this work presents the experimental characterization of the operating temperature and output power from irrigated 255 W PV panels. The experiment considered twelve irrigation regimens with four flow rates (1.75 l/min, 3.75 l/min, 4.75 l/min, and 9.50 l/min) and four operating cycles (1':29', 5':25', 15':15', and continuous). The study provides a description of transient cooling processes as functions of flow rate and solar irradiation, as well as heating of the PV panel. Such description is based on data analysis using two indices: relative temperature difference (RTD) and generated power increase (GPI), which quantifies the additional generated energy and estimates the net energy benefit considering the energy consumed by the irrigation system. Results indicate that irrigation can enhance daily energy production by 10%; a flow rate equal to or greater than 3.75 l/ min (2.34 l/min/m^2) produces similar effects. The GPI caused by irrigation depends on the solar irradiation, where GPI is found to be 0.5% to 2.0% for 400 W/m^2 or lower, 2% to 5% for values between 400 W/m^2 and 800 W/m^2, and 5% to 10% for 800 W/m^2 or greater. The power consumed by the irrigation system significantly affects the net energy benefit.

1. Introduction

PV systems are a green energy strategy with great popularity around the world due to their easy installation, operation, maintenance, and recent substantial reduction in cost ($/Wh). They consist mainly of PV panels and management units (inverters or controllers).

These systems have low average energy conversion efficiency that varies between 10% and 16% (Nižetić et al., 2018), which is due mostly to the power conversion principle in PV cells and the thermal effects from which they suffer. Such effects are caused primarily by incident solar irradiation and the surrounding air temperature (a Hussien et al., 2015; Molki, 2011). Excess heat stored in PV modules causes an undesirable increase in operating temperature and a resulting reduction in output power, particularly for Si-based PV panels (monocrystalline and polycrystalline) (Nižetić et al., 2018; Zilli et al., 2018).

This thermal effect is significant and predictable; experiments with (Si-based) PV panels show that losses ranging from 0.25% to 0.50% per °C (Smith et al., 2013, 2014; Ju and Fu, 2011; Nižetić et al., 2016). This demonstrates the inverse relationship between energy conversion efficiency and the operating temperature (Kane et al., 2017).

Reindl et al. (2012) warned about the need for mitigating the operating temperature of PV panels in tropical warm climates, since the high incident solar irradiation can reduce the annual

* Corresponding author.
E-mail address: gealosma@uis.edu.co (G. Osma-Pinto).

https://doi.org/10.1016/j.egyr.2019.04.010

energy production by approximately 10%, although output power can fall up to 20% when solar irradiation is greater than 700 W/m^2.

These power losses can be mitigated with some cooling strategies, including placing a green roof below the PV panels (Nagengast et al., 2013; Chemisana and Lamnatou, 2014), ventilation (Teo et al., 2012), using a heater exchanger (Ebaid et al., 2018; Hussien et al., 2015), evaporative cooling from sprinkling water (Zilli et al., 2018; Bai et al., 2016; Wang et al., 2018; Alami, 2014), and forced irrigation on the front surface of the PV panel (Ju and Fu, 2011; George et al., 2013; Bahaidarah et al., 2013; Odeh and Behnia, 2009; Meyer and Busiso, 2012; Kordzadeh, 2010), among others.

Heat extraction from a PV panel using water is a more complex solution than ventilation or the use of a green roof, although it can be more effective (a Hussien et al., 2015). In general, cooling methods based on water provide larger increases in the power output from PV panels, ranging from 10% to 20% during peak irradiance (i.e., near noon) (Nižetić et al., 2018).

Irrigation allows one to reduce heat stored into the PV panel due to heat transfer by convection between flowing water and the front surface of the PV panel. This reduces the operating temperature of the PV panel and, resulting in increased output power (a Hussien et al., 2015).

A water film on front surface of a PV panel significantly reduces its operating temperature when solar irradiation is high, e.g., from 54 °C to 24 °C (Nižetić et al., 2016), which can improve the output power from 15% to 20% (Nižetić et al., 2016; Habiballahi et al., 2015). These improvements are lower when solar irradiation diminishes.

Table 1 shows some prior experimental research that investigated irrigated PV panels using water as a coolant. Several of these studies were conducted in temperate locations and, in general, analyse the behaviour of PV panels at low and middle nominal power output (53 W–185 W) for several flow rates (1.4 l/min/m^{2}to 15.9 l/min/m^2). The daily energy generation improvements vary mostly from 4% to 10% during continuous operation (3 to 10 h), although such improvements can range between 0.7% and 27.6%.

Saxena et al. (2018) present a laboratory experiment where two 40 W PV panels were irrigated at flow rates of 3.0 l/min (12.5 l/min/m^2), 5.3 l/min (22.1 l/min/m^2), and 6.2 l/min (25.8 l/min/m^2). Irrigation was applied intermittently in order to ensure that irrigation began when the operating temperature reached 40 °C and ended when this temperature descended to 30 °C. This operation cycle increased the generated energy by up to 17.9%.

Apart from experimental studies, Odeh and Behnia (2009) and Schiro et al. (2017) focused on modelling the irrigation effect and Sargunanathan et al. (2016), Siecker et al. (2017), and Nižetić et al. (2018) presented reviews of cooling methods for PV panels involving the use of a water film on the front surface of a PV panel.

Prior research results (Odeh and Behnia, 2009; Kordzadeh, 2010; Habiballahi et al., 2015; Moharram et al., 2013; Tomar et al., 2018; Sainthiya et al., 2018; Saxena et al., 2018; Ramkumar et al., 2016) indicate that an irrigation system can operate with continuous or intermittent cycles and consists mainly of a water provider, pump, tank, data logger, pyranometer, several temperature sensors for the PV panels and air, and an anemometer. The data sampling can be mostly between 1 and 15 min.

The water provider is located on top of PV panel and a water film flows downward due to gravity (Krauter, 2004); water could be applied using nozzles (Krauter, 2004), trickling tube (Odeh and Behnia, 2009), sprays of water (Nižetić et al., 2016), PVC pipes with holes (Smith et al., 2014; Sainthiya et al., 2018), or water droplets (Moharram et al., 2013).

Some irrigation systems can be used to control the maximum and minimum operating temperature values of the PV panels (Wang et al., 2018; Moharram et al., 2013; Saxena et al., 2018) or water temperature (Nižetić et al., 2016; Moharram et al., 2013); however, most experiments do not have control over these variables.

Based on recent research, it possible to show that irrigation over the front surface is one of the most promising methods for cooling PV panels. Nevertheless, most studies describe a broad range of increased energy production values (from 0.7% to 27.6%) considering temperate climate conditions, which makes it difficult to reliably estimate the impact of irrigation of PV panels in tropical locations.

Thus, it is necessary to conduct more experiments for estimating the energy benefits of PV panels due to discontinuous operation cycles for several irrigation flow rates and solar irradiation levels in warm or tropical places. To make such estimation, it is necessary to consider technical characteristics of the irrigation system, mainly operation cycle and flow rate, and the climate conditions, as solar irradiance and ambient temperature. So, there is a gap in the literature with respect to the analysis of the impact of these factors on energy benefit produced by an irrigation system on PV panels. This study aims to fill this gap by investigating the heat transient processes (cooling and heating) caused by the irrigation, the correlation between flow rate and solar irradiance with output power increase, and the influence of the operation cycle on the increased energy production, considering tropical climate conditions.

This work presents an experimental study of irrigation of PV panels in Bucaramanga (Colombia), whose tropical climate causes changes in the operating temperature that can reduce the output power by up to 15% near noon (10 a.m. to 2 p.m.) throughout most of the year. Specifically, we studied the effect of twelve irrigation regimens on 255 W PV panels, which were operated using microinverters (Enphase M250). The effect of four flow rates (1.75 l/min, 3.75 l/min, 4.75 l/min, and 9.50 l/min) and four operation cycles (1′:29′, 5′:25′, 15′:15′, and continuous) were examined. An analysis of the results allows us to describe the transient behaviour of the operating temperature and output power during cooling and heating processes using two indices (*TRD* and *GPI*), the effect of solar irradiation level, and the effect of residual water evaporation on the front surface of the PV panel, and to obtain an estimate of the energy benefits provided by irrigation.

2. Experiments

This section describes the experimentation site, PV system we used, irrigation system, monitoring system, indices for characterizing the effect of irrigation on PV panels, and considerations for estimating the net energy benefit provided by irrigation.

2.1. Place of experimentation

Experiments were conducted in the Edificio de Ingeniería Eléctrica (EIE) of the Universidad Industrial de Santander (UIS). This university is located at 7.13° North latitude and 73.13° West longitude, in Bucaramanga (Colombia). This city has warm climate and is 960 masl (Vergara-Barrios et al., 2014; Osma-Pinto et al., 2015). Table 2 presents general climate data of this tropical city. The EIE building is a pilot green building and provides an ideal location to research on energy use in warm tropical conditions, such as green roofs, daylighting, natural ventilation, building automation, and PV generation.

Table 1
Some experimental results regarding the effect of irrigation on the power output from PV panels.

Ref.	Latitude (°) Country	Power panel (W)	Flow rate (l/min/m^2)	Operation cycle (t_a: t_b)	Increment (%)
Krauter (2004) (2004)	−22.9° Brazil	53	4.4	Continuous 7 a.m. to 5 p.m.	10.3%
Odeh and Behnia (2009) (2009)	32.0° Jordan	60	9.6	Continuous 6 a.m. to 7 p.m.	4%–10%
Kordzadeh (2010) (2010)	30.3° Iran	90–135	0.54–5.46	Continuous 7 a.m. to 3 p.m.	0.7%–3.7%
Moharram et al. (2013) (2013)	30.1° Egypt	185	3.9	Discontinuous (5′: 15′)	9% (max.)
Smith et al. (2014) (2014)	45.5° USA	175	5.2	Continuous 11:10 a.m. to 5:30 p.m.	9.4%
Habiballahi et al. (2015) (2015)	30.3° Iran	135	2.5–4.3	Continuous 8 a.m. to 5 p.m.	12.9%–23.3%
Nižetić et al. (2016) (2016)	43,5° Croatia	50	7.74–12.10	Continuous 11 a.m. a y 2 p.m.	16.3%
Tomar et al. (2018) (2018)	28.6° India	75–90	4–7	Continuous 7 a.m. a y 5 p.m.	6.6%–7.8%
Sainthiya et al. (2018) (2018)	26.9° India	75	1.4–3.5	Continuous 8:30 a.m. to 5:00 p.m.	27.6%

Table 2
General climate data from Bucaramanga.

Parameter	Value
Average annual precipitation	1279 mm
Average ambient temperature	24 °C (During the day) 27 °C (During the sunlight hours)
Average maximum temperature	31 °C
Average solar irradiation	4.8 kWh/m^2/day
Wind speed	1.0–1.5 m/s

Table 3
Guaranteed measurement error for the used measuring equipment.

Sensor type	Measurement error
Pyranometer	±0.2%
Temperature	±0.5%
Air velocity	±3.0%
DC electrical power	±0.5%
AC electrical power	±0.2%

2.2. PV system

PV panels P5, P6, and P7 of Module 1 of the PV system installed on green roof of the EIE Building were selected for examination. This module consists of 255 W, 1.6 m^2 polycrystalline PV panels CS6P-255 (Canadian Solar) with 16% power conversion efficiency. These panels are managed using microinverters (Enphase M250), which encourage an individual analysis of the behaviour of each PV panel and ensure operation at the maximum power point. The PV system injects generated power into a low voltage network in the building (3φ - 4 wires to 120 V/208 V).

2.3. Monitoring

The monitoring system allows to measure various climate variables (solar irradiation, air temperature, and air velocity) and the operating temperature of the PV panels. This system consists of a pyranometer (Kipp&Zonen SMP-11), three air velocity sensors (EE576, EE671, and DC-12), thermocouples K-type, and three data loggers (OMEGA OM-CP-OCTTEMP2000, PACE XR5-SE-20 mV, and CAMPBELL CR800X). The pyranometer (Pi) was installed in the same working surface as the PV panels, which have an inclination of 10° with Southern orientation. Six thermocouples (T1–T6) were used to measure the temperature on the back surface of the PV panels and were located at 1/4 (0.40 m) and 3/4 (1.20 m) along the length (1.60 m) of the PV panel; another four thermocouples were installed to monitor the ambient temperature (Ta_1, Ta_2, and Ta_3) and the water irrigation (T_w). The sensors SV1, SV2, and SV3 allow to measure the air velocity over and under of the PV panels. Fig. 1 shows the top view of the PV panels above the green roof with the locations of some installed sensors.

Three DC energy metres (AcuDC243, Class 0.5 in power) and one AC energy metre (Acuvim IIR, Class 0.2 in power) were used for measuring the electrical variables of the PV panels and microinverters. These metres were installed into electrical boards above the terrace next to overcurrent protection.

Table 3 presents the guaranteed measurement error according to the technical sheet data of equipment producers. Most variables were sample in 1 min intervals; meanwhile, electrical variables and operating temperature were sample in 10 s intervals.

2.4. Irrigation system

Fig. 2 shows a schematic diagram (cross-sectional view) of the irrigation system components of used for characterizing the effect of the water flow rate on the output power from PV panels P5, P6, and P7 during the operation cycle. This system consists of a tank, submergible pump, PVC supply pipeline, collecting PVC pipeline, water provider, relay, and controller; these latter two components allow to control the operation cycle of the pump. Also, this figure illustrates the locations of several installed sensors belonging to the monitoring system. Fig. 3 shows the irrigation system implemented over terrace.

The experiment allowed us to investigate twelve irrigation regimens (A to L) considering the eleven cases (I to XI) presented by Table 4. Each regimen is defined in terms of the water flow rate during irrigation (l/min or l/min/m^2) and the operation cycle t_a: t_b, where t_a is the irrigation time and t_b is the non-irrigation time in 30 min intervals. The variety of regimens and time intervals facilitates investigation of the transient cooling and heating processes in an irrigated PV panel.

In this experiment, the temperature of the irrigation water varies as the day progresses. At sunrise, this temperature is equal

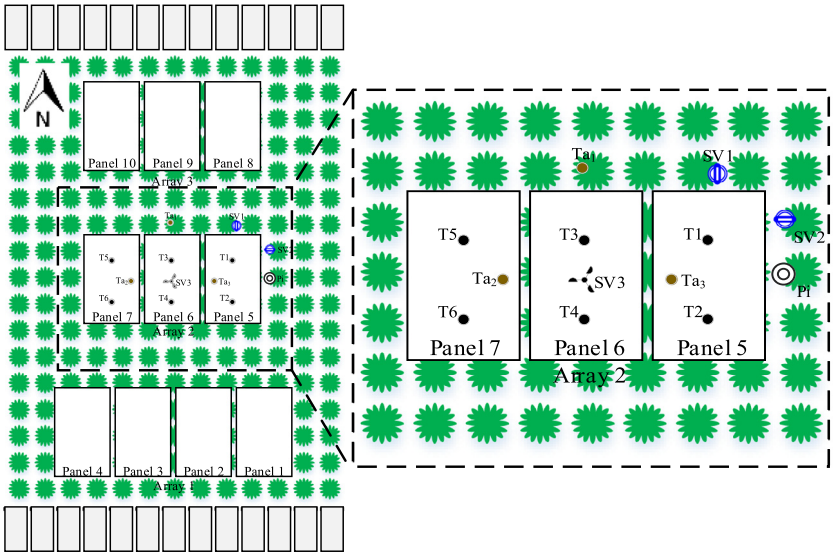

Fig. 1. Top view of the PV panels above the green roof with the locations of some sensors installed for monitoring climatic variables and operating temperature of the three PV panels. (For interpretation of the references to colour in this figure legend, the reader is referred to the web version of this article.)

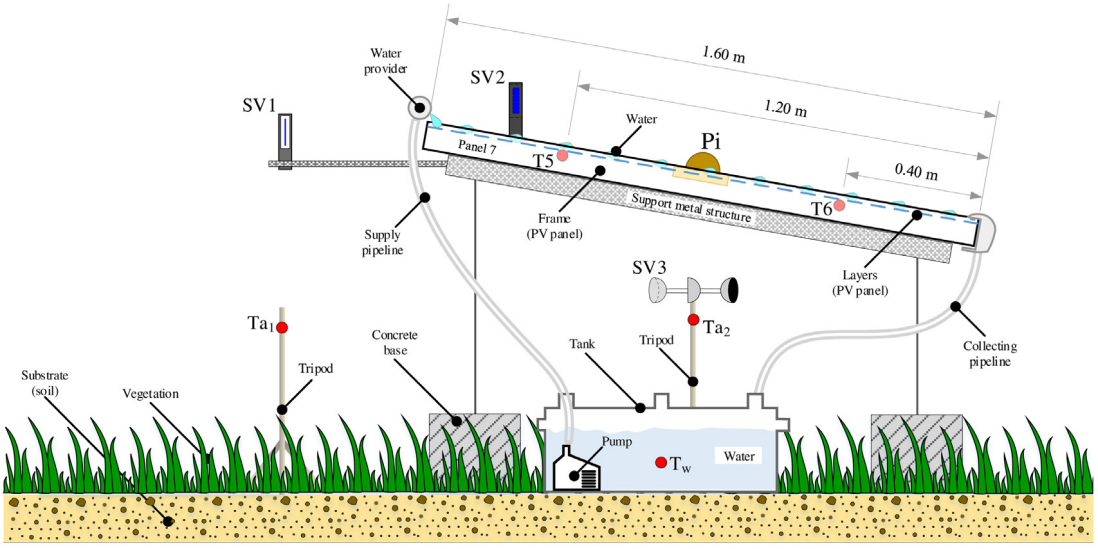

Fig. 2. Cross-sectional view of the PV panels above green-vegetated roof showing the components of the irrigation system and the position of some sensors installed for monitoring climatic variables and operating temperature of the PV panel P7. (For interpretation of the references to colour in this figure legend, the reader is referred to the web version of this article.)

Table 4
List of cases studied involving three PV panels (P5, P6, and P7).

Case	PV panel P5	PV panel P6				PV panel P7			
		Regimen	t_a: t_b	Flow rate		Regimen	t_a: t_b	Flow rate	
I		A	15′:15′	9.50 l/min	5.94 l/min/m^2	B	1′:29′	9.50 l/min	5.94 l/min/m^2
II		I	15′:15′	3.75 l/min	2.34 l/min/m^2	A	15′:15′	9.50 l/min	5.94 l/min/m^2
III		I	15′:15′	3.75 l/min	2.34 l/min/m^2	L	15′:15′	1.75 l/min	1.09 l/min/m^2
IV		J	1′:29′	3.75 l/min	2.34 l/min/m^2	K	1′:29′	1.75 l/min	1.09 l/min/m^2
V	Without irrigation	F	1′:29′	4.75 l/min	2.97 l/min/m^2	H	15′:15′	4.75 l/min	2.97 l/min/m^2
VI	(reference)	J	1′:29′	3.75 l/min	2.34 l/min/m^2	B	1′:29′	9.50 l/min	5.94 l/min/m^2
VII		G	Cont.	4.75 l/min	2.97 l/min/m^2	C	Cont.	9.50 l/min	5.94 l/min/m^2
VIII		E	5′:25′	4.75 l/min	2.97 l/min/m^2	C	Cont.	9.50 l/min	5.94 l/min/m^2
IX		F	1′:29′	4.75 l/min	2.97 l/min/m^2	C	Cont.	9.50 l/min	5.94 l/min/m^2
X		B	1′:29′	9.50 l/min	5.94 l/min/m^2	C	Cont.	9.50 l/min	5.94 l/min/m^2
XI		D	5′:25′	9.50 l/min	5.94 l/min/m^2	C	Cont.	9.50 l/min	5.94 l/min/m^2

to ambient temperature; later, it can increase according to ambient temperature variation, heat extraction from the PV panel, and heat transfers between water and surrounding. Two 22 W submergible pumps with regulation taps provided four flow rates (1.75 l/min, 3.75 l/min, 4.75 l/min, and 9.50 l/min) during the experiment. The flow rate of 1.75 l/min was insufficient for

Fig. 3. Irrigation system with two PV panels (P6 and P7) installed on the green roof together with some components of the monitoring system. (For interpretation of the references to colour in this figure legend, the reader is referred to the web version of this article.)

creating a water film over the PV panels. An Arduino module and two relays were used to control and actuate the pumps. A 40 L cava (tank) of expanded polystyrene was used as a tank in order to avoid the heating due to incident solar irradiation.

P5 operated with no irrigation and functioned as a reference PV panel for analysing the effect of irrigation on panels P6 and P7.

Although the experiment used the same models for the PV panel and microinverters, the analysis began with an adjustment process for the output power data obtained from each PV panel and its coupled microinverter. This consisted of installing and monitoring the PV panels under same conditions and studying their individual behaviour. The results indicate the existence of slight differences (<1%) output power when they were not irrigated. However, in order to improve the quality of the experimental data, the analysis involved normalizing the data with respect to one of the three PV panels and its microinverter.

2.5. Characterizing the irrigation effect

Analysing the effect of irrigation on the PV panels is based on measuring variations in the operating temperature and output power. The solar irradiation level influences the operating temperature and the output power simultaneously, and that former variable affects the latter. Thus, is not possible to generalize the irrigation effect at all times. For that reason, we introduce the temperature relative difference (*TRD*) and generated power increase (*GPI*) indices.

The *TRD* index varies for all time and is calculated using Eq. (1), where T_{P_Ir} is the temperature of the irrigated PV panel, T_{amb} is the ambient temperature, and T_{P_NoIr} is the temperature of the non-irrigated PV panel. This index can take values between 0.0 and 1.0, where 0.0 is the best scenario and indicates that the irrigated PV panel has a temperature equal to the ambient temperature, thus generating the maximum output power for these climate conditions. Meanwhile, a value of 1.0 is the worst scenario and means that an irrigated panel has the same temperature as a non-irrigated PV panel (reference), thus, there is no additional output power.

$$TRD = \frac{T_{P\_Ir} - T_{P\_amb}}{T_{P\_NoIr} - T_{P\_amb}} \tag{1}$$

Index *GPI* describes the percentage change in output power with respect to the more unfavourable condition and is defined in Eq. (2), where P_{gen_Ir} is the generated output power when the PV panel is irrigated and P_{gen_NoIr} is the generated output power when the PV panel is not irrigated.

$$GPI = \frac{P_{gen\_Ir} - P_{gen\_NoIr}}{P_{gen\_NoIr}} \tag{2}$$

2.6. Estimation of the energy benefit provided by irrigation

The net energy benefit (*NEB*) generated by the irrigation system is defined as the difference between the additional generated energy (E_{add}) provided by irrigation and the energy consumed by the irrigation system per PV panel (EC_{IS}). E_{add} and EC_{IS} can be estimated from sampling the power value collected by the monitoring system, as shown in Eqs. (3) to (4). EC_{IS} is equal to the sum of energy consumed by the controller per PV panel (E_{cont}/n_{PV}) and energy consumed by the water pump (E_{wp}); therefore, it depends on the controller power (P_{cont}), the operation time of the controller ($t2 - t1$), the number of the PV panels (n_{PV}), the submergible pump power (P_{wp}), and the total irrigation time ($Nt \cdot t_a$), where Nt is the number of irrigation intervals.

$$Eadd \approx \sum_{i=1}^{Nt} \left(p_{gen\_Ir}\,(i) - p_{gen\_NoIr}\,(i)\right) \Delta t \tag{3}$$

$$EC_{IS} = E_{wp} + E_{cont}/n_{PV} = P_{cont}\,(t2 - t1)/n_{PV} + P_{wp} \cdot Nt \cdot t_a \tag{4}$$

3. Results and discussion

This section presents a description of the irrigation effect using thermograms and variations in the operating temperature and output power during specific time windows for a specific case in Table 4. The effect of irrigation based on the *TRD* and *GPI* indices is examined, the duration of cooling and heating processes in an irrigated PV panel are analysed, and the energy benefit due to irrigation is estimated.

3.1. Description of the irrigation effect using thermograms – case V

Fig. 4 shows thermograms that allow to visualize variations in water temperature and operating temperature of the irrigated PV panels. Panels P6 (middle) and P7 (left) are examined with respect to panel P5 (right). Panels P6 and P7 are irrigated using regimens F (1′:29′, 4.75 l/min) and H (15′:15′, 4.75 l/min), respectively.

Panels P5 and P6 have the same operating temperature at $t = -5$ s due to the fact that irrigation has already ceased on P6. However, this effect still slightly impacts P7 since its temperature is 3 °C below the temperature of P5. At $t = 1$ s, the water moves irregularly over P6 and P7, although seconds later the water film becomes uniform. At $t = 60$ s, the temperature of P6 and P7 decrease from 45 °C to 30 °C, at which point irrigation of panel P6 ends. These results indicate that irrigation produces a quick transient for both the operating temperature and output power, especially during the first minute. At $t = 300$ s, panel P7 is still irrigated and its operating temperature is around 30 °C. Meanwhile, panel P6 exhibits a slightly higher temperature of about 34 °C or 35 °C, as its irrigation regime finished about 4 min prior.

On the other hand, results indicate that water into the tank suffers an increment of temperature around to 6 °C due to the removed heat from PV panel, shifting from 27 °C to 33 °C for the tank of P6. It is important to note that the temperature of the irrigation water varies as the day progresses in this experiment, due to ambient temperature variation, heat extraction from the PV panel and heat transfers between water and surrounding. This temperature can be controlled and its effect analysed in a next study.

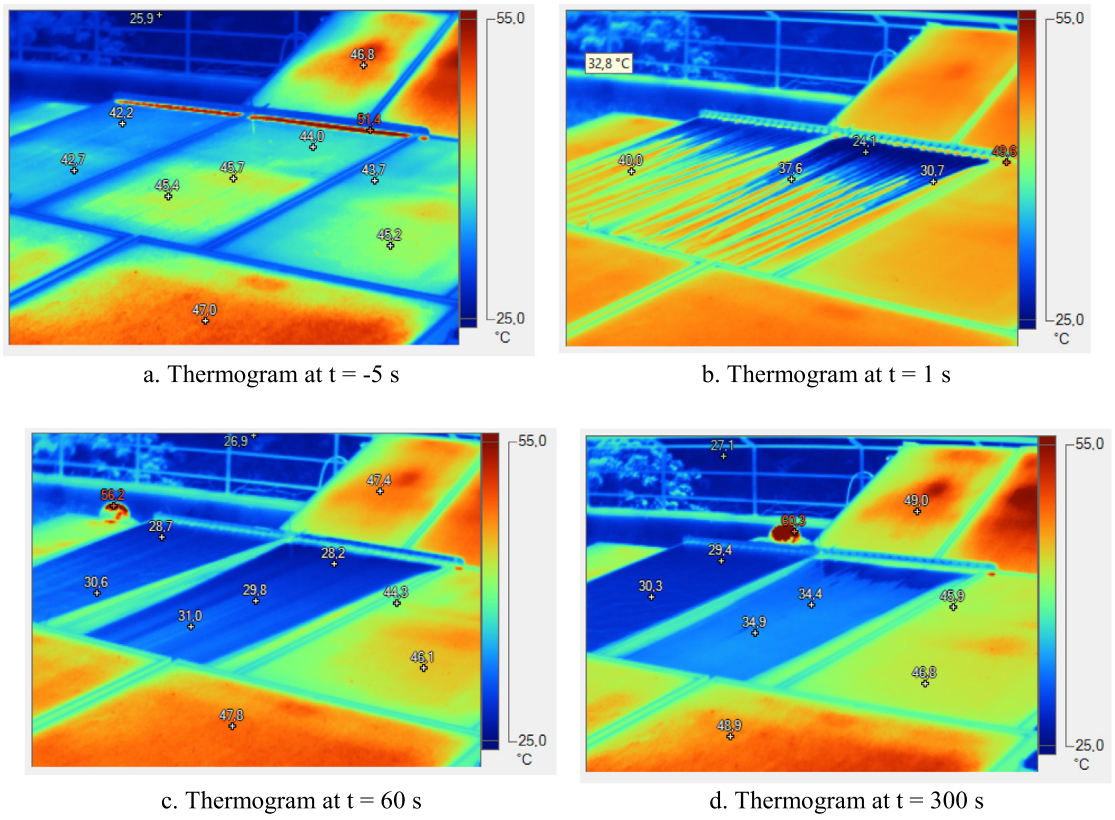

a. Thermogram at t = -5 s

b. Thermogram at t = 1 s

c. Thermogram at t = 60 s

d. Thermogram at t = 300 s

Fig. 4. Thermograms showing the evolution of water temperature and operating temperature over 300 s.

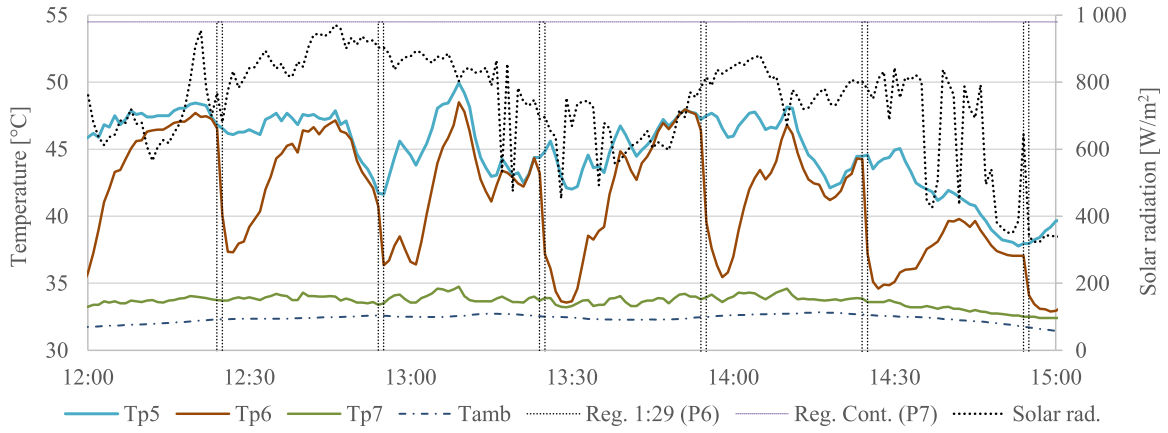

Fig. 5. Operating temperature of the PV panels.

3.2. Description of the variation of the operating temperature and output power based on use of the TDR and GPI indices – case X

Next, Case X is analysed based on monitoring data, where panels P6 and P7 were irrigated according to regimens B (1′:29′, 9.50 l/min) and C (30′:0′, 9.50 l/min), respectively.

Effect on the operating temperature of the irrigated PV panels

Fig. 5 shows the operating temperature over time for three PV panels. The temperatures of the irrigated PV panels (*Tp6* and *Tp7* for panels P6 and P7, respectively) fluctuate between ambient temperature (dashed–dotted line), which is the minimum temperature that a PV panel during irrigation, and the temperature of panel P5 (*Tp5*, blue line), which is the maximum temperature that a PV panel can reach.

Constant irrigation kept the temperature of panel P7 very close to ambient temperature; the temperature of panel P7 is slightly larger than ambient because water is heated due to continuous heat extraction from P7 during irrigation.

On the other hand, *Tp6* decreased quickly during the first minute of irrigation and approached *Tp7*. In addition, panel P6 continues its cooling process for 1 to 5 min after irrigation ends due to evaporation of the residual water film that formed over the front surface of the PV panel at $t = 60$ s.

The curves $\Delta Tp5p6$ and $\Delta Tp5p7$ in Fig. 6 show that the operating temperature decreased due to the irrigation regimen in panels P6 and P7 relative to P5. The temperature decrease varies between 6 °C and 15 °C for panel P7 and between 0 °C and 12 °C for panel P6.

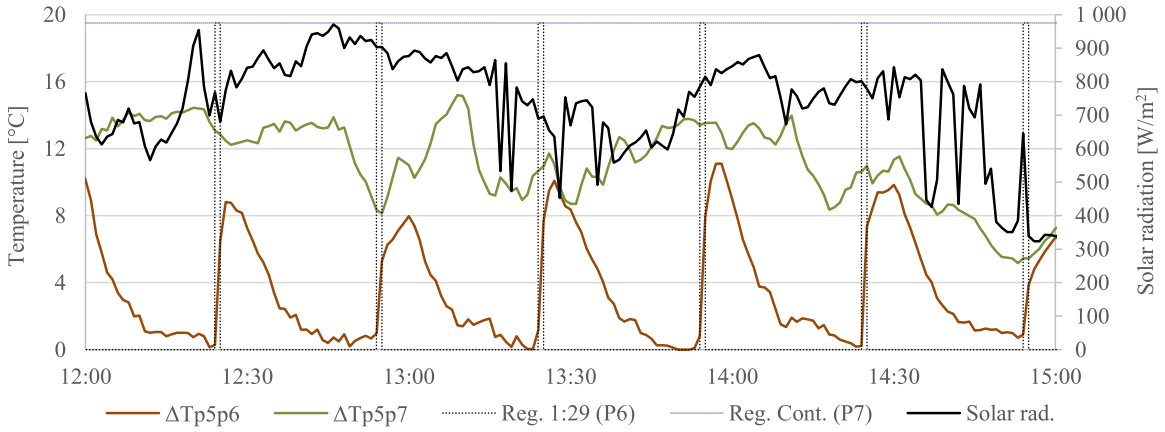

Fig. 6. Decrease in the operating temperature for the irrigated PV panels (P6 and P7).

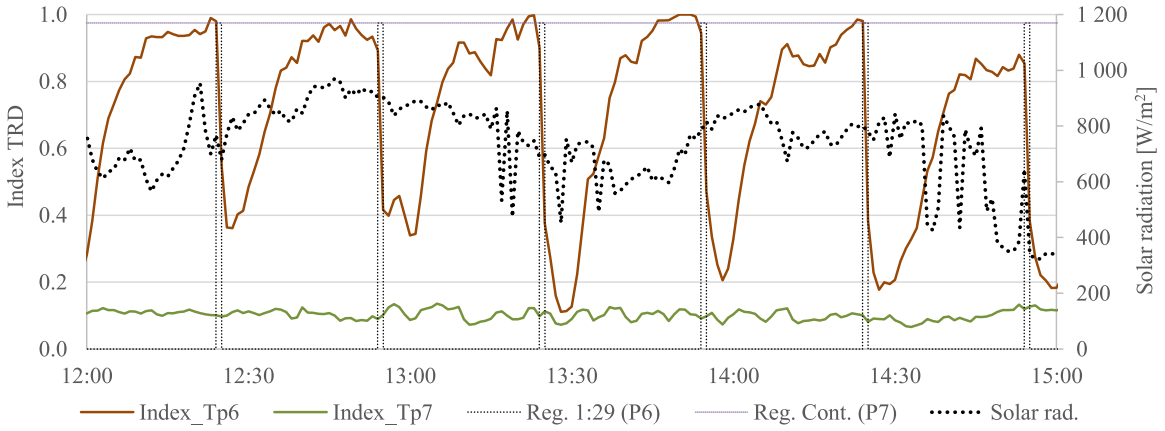

Fig. 7. *TRD* over time for the irrigated PV panels (P6 and P7).

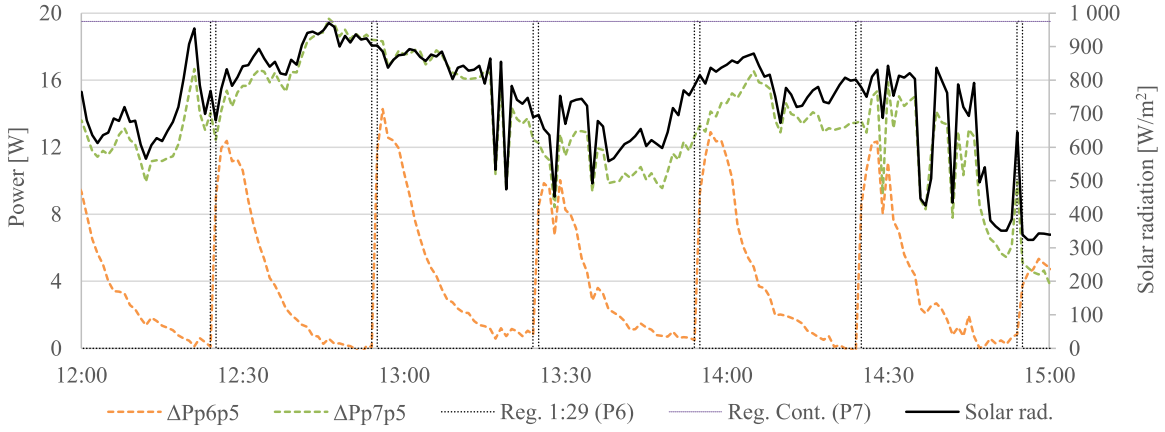

Fig. 8. Increasing output power generated by the irrigated PV panels.

Variations in operating temperature can vary between 0 °C and 35 °C. However, these variations cannot be generalized because they depend on solar irradiation and the operating temperature of the reference PV panel. This is more critical for tropical places, such as Bucaramanga, due to fluctuating solar irradiation and clouds. For that reason, the temperature variation is normalized using *TRD*.

Fig. 7 shows the *TRD* index over time for panels P6 and P7. Before each beginning irrigation, *TRD* for P6 is approximately 1.0 as the effect produced from the previous irrigation cycle has vanished, although this value decreases quickly to between 0.2 and 0.4 at $t = 60$ s. In panel P7, *TRD* varies from 0.10 to 0.20 as the water temperature during irrigation is higher than ambient temperature.

Effect of irrigation on output power

Fig. 8 shows the output power $\Delta Pp6p5$ and $\Delta Pp7p5$ with respect to P5 for panels P6 and P7, respectively. Panel P7 exhibits a maximum power output increase of 19.5 W during the displayed time window due to continuous irrigation, where the incident solar irradiation was 950 W/m^2. On the other hand, $\Delta Pp6p5$

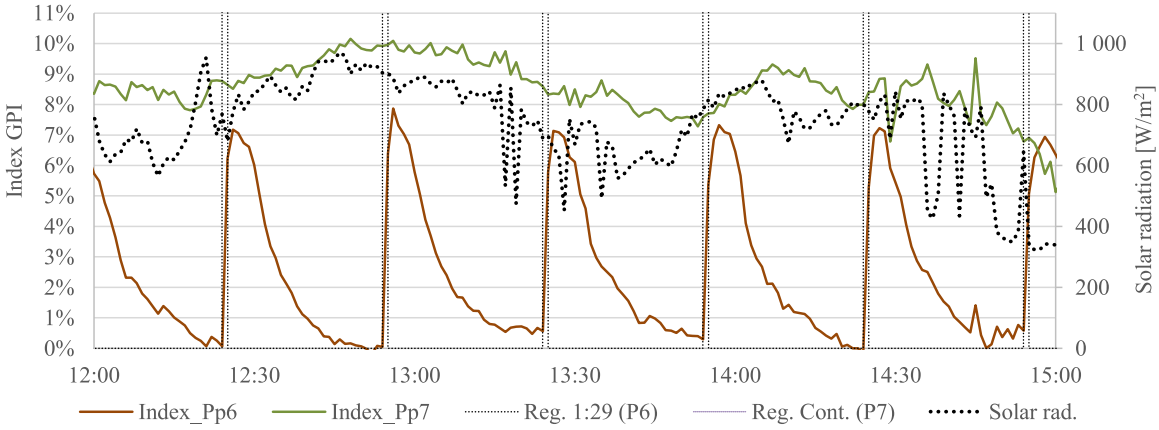

Fig. 9. GPI over time for irrigated PV panels P6 and P7.

describes the effect of thermal transients (cooling and heating) over output power. The cooling transient occur during the first 5 min and is faster than the heating transient, which occurs from $t = 5$ min to $t = 30$ min.

Fig. 9 shows the *GPI* index over time. These data allow us to generalize the increased output power from panels P6 and P7 with respect to P5, whose greatest values were 8% and 10%, respectively. In contrast to *TDR*, solar irradiation significantly influences *GPI*; high solar irradiation (e.g., from 10 a.m. to 2 p.m. without clouds) can produce average *GPI* values between 7% and 10% and maximum values up to 15%. Meanwhile, for low solar irradiation (before 9 a.m. and after 4 p.m.) produces *GPI* values ranging from 0% to 3%.

3.3. Influence of irrigation regimens on TRD and GPI indices

Fig. 10a and b show the normalized thermal behaviour of a PV panel due to irrigation for several solar irradiation levels. In general, typical *TRD* behaviour occurs for solar irradiation values greater than 200 W/m^2. When solar irradiation is less than 200 W/m^2, the cooling and heating transients are slow and this case could be disregarded for generation analysis due to the low energy contribution.

The *GPI* shown in Fig. 10c and d indicate that the increased output power is directly related to the solar irradiation level. Fig. 10e and f show daily averages of the indices for both regimens. The average *GPI* index is very close to characteristic *GPI* curve for solar irradiation ranging from 400 W/m^2 to 600 W/m^2, which covers the average solar irradiation for Bucaramanga (417 W/m^2 from 6 AM to 6 PM). These curves show the transient cooling and heating processes that a PV panel can experiment and describe an inverse relation between *TRD* and *GPI*. For example, the curves of Fig. 10e can be correlated between them by a linear function with negative slope, as shown in Fig. 11, where GPI_{ex} represents data test, GPI_{lin} corresponds to the linear trend line, and GPI_{linap} is an approximation of GPI_{lin}. GPI_{lin} is presented by Eq. (5) with $R^2 = 0.92$ and an estimation error of *GPI* value of 10.4% (NRMSE). GPI_{linap} is an alternative lineal function shown by Eq. (6) that can be determined with only two points, ($TRD = 1$; $GPI = 0\%$) and (TRD_{min}; GPI_{max}), where $GPI_{linap} = a \cdot (TRD - 1)$ and $a = -GPI_{max}/(1 - TRD_{min})$; which allows to estimate *GPI* value with an error of 14.8% (NRMSE).

$$GPI_{lin} = -7.86 \cdot TRD + 8.20\ (\%) \tag{5}$$

$$GPI_{linap} = -9.44 \cdot TRD + 9.44\ (\%) \tag{6}$$

In order to analyse the effect of flow rate on the thermal behaviour of a PV panel, Fig. 12 shows averages *GPI* indices over time as a function of operation cycle (1′:29′, 5′:25′, 15′:15′, and continuous) and allows to appreciate that the flow rate determines the maximum *GPI* value. Fig. 12a shows the impact of operation cycles of 1′:29′, where regimens B (9.50 l/min), F (4.75 l/min) and J (3.75 l/min) produce maximum output power increases of 6%–7%, while Regimen K (1.75 l/min) only increases the output power by up to 3%. For regimens with operation cycle of 5′:25′, Fig. 12b shows a maximum increment near 7% for Regimen D (9.50 l/min) and Regimen E (4.75 l/min). Fig. 12c shows that flow rates of 3.75 l/min (Regimen I), 4.75 l/min (Regimen H), and 9.50 l/min (Regimen A) produce the similar effect in the 15′:15′ operation cycle, producing maximum output power increases of 7–8.5% for. Despite the fact that a flow rate of 1.75 l/min (Regimen K) yields a reduced thermal effect, it can increase the generated energy by up to 6% because the irrigation time (15′) is long enough to extract a significant amount of heat stored in a PV panel during the first 10 min. Regimens C and G (continuous irrigation) produce increased daily energy generation near 8% and 6.5%, respectively, as shown in Fig. 12d. Clearly, *GPI* tends to be insensitive to flow rates equal to or greater than 3.75 l/min.

Fig. 13 shows the average *TRD* and *GPI* indices for four operation cycles. In general, continuous irrigation provides a *TRD* value of 0.2 and produces an energy increase near 8%. The maximum *GPI* values are 5.6% ($t = 3$ min), 6.8% ($t = 6$ min), and 7.4% ($t = 17$ min) in the 1′:29′, 5′:25′, and 15′:15′ operation cycles, respectively. These values were obtained due to evaporative cooling after irrigation ended.

It is important to note that values obtained for *TRD* and *GPI* are referenced to the thermal and electrical behaviour of panel P5 (i.e., the non-irrigated PV panel), which was installed over a green roof and with wind speed between 0 m/s and 1 m/s. Therefore, it is possible to obtain higher *GPI* values for PV panels installed on a concrete roof, although water could not be used to irrigating vegetation in this case.

3.4. Length of the cooling and heating processes in an irrigated PV panel

During an operation cycle (t_a: t_b) in the irrigation system, an irrigated PV panel exhibits cooling and heating transient processes. Cooling occurs in two stages: direct cooling and indirect cooling.

Direct cooling occurs while a water film runs over the front surface of a PV panel and extracts stored heat. This stage lasts t_a minutes and quickly reduces the operating temperature of the PV panel, which has behaviour similar to a discharging capacitor. Consequently, it is possible to estimate the time constant of direct cooling (τ_{dc}). Results indicate that τ_{dc} depends on the flow rate. Specifically, this constant takes values around 40 s, 50 s, 60 s,

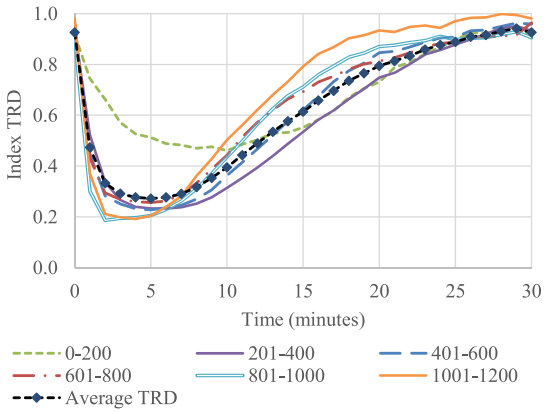

a. DRT with Regimen B for 0-200, 201-400, 401-600, 601-800, 801-1000, and 1001-1200 W/m^2.

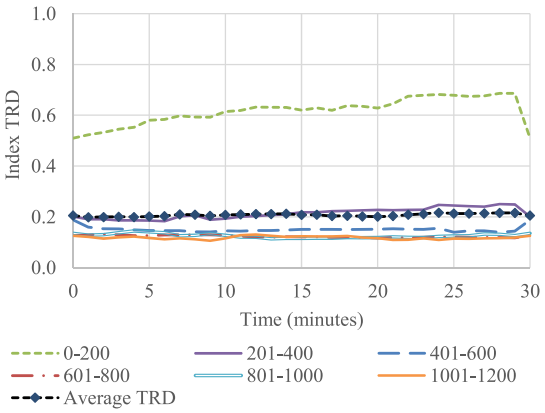

b. DRT with Regimen C for 0-200, 201-400, 401-600, 601-800, 801-1000, and 1001-1200 W/m^2.

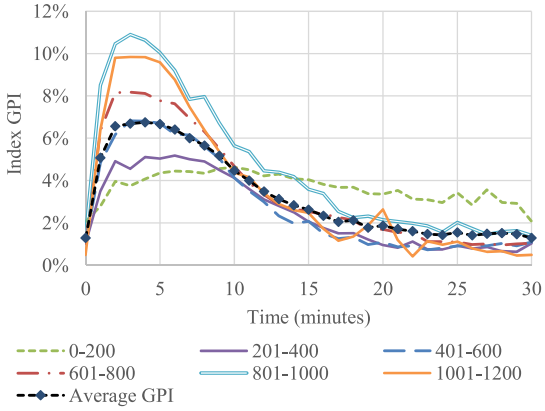

c. GPI with Regimen B for 0-200, 201-400, 401-600, 601-800, 801-1000, and 1001-1200 W/m^2.

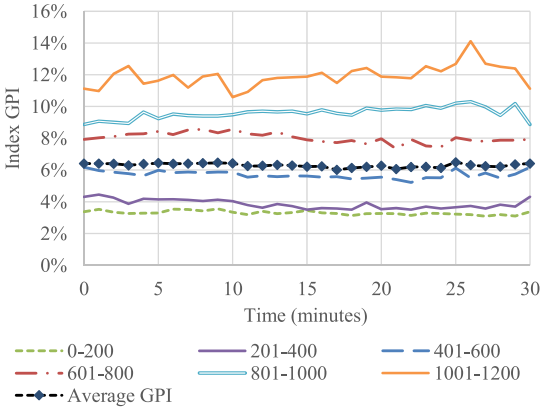

d. GPI with Regimen C for 0-200, 201-400, 401-600, 601-800, 801-1000, and 1001-1200 W/m^2.

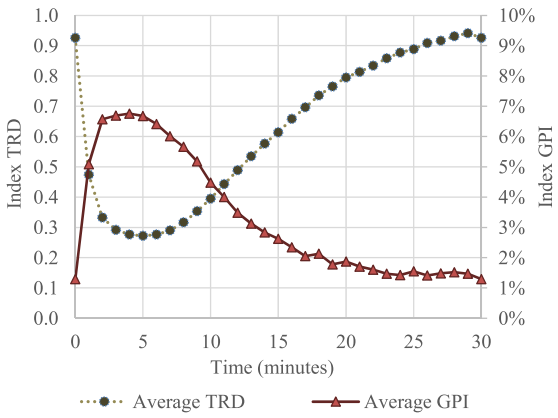

e. Average TRD and GPI indices for Regimen B.

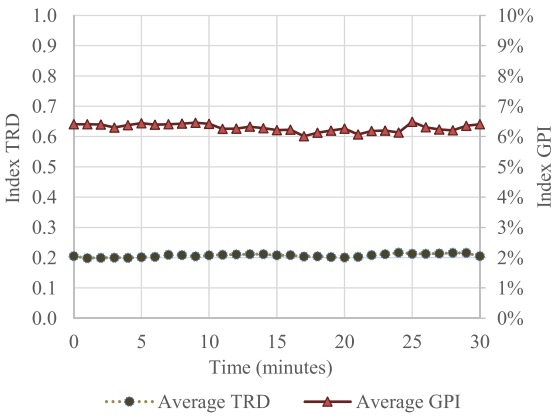

f. Average TRD and GPI indices for Regimen C.

Fig. 10. *TRD* and *GPI* indices for regimens B and C at several solar irradiation levels (Case X).

and 150 s for flow rates of 9.50 l/min, 4.75 l/min, 3.75 l/min, and 1.75 l/min, respectively, as shown in Fig. 14. One can see that a flow rate of 3.75 l/min or greater produces a similar decrease in the operating temperature of an irrigated PV panel. This datum is essential for selecting a low power pump and, thus, reducing the energy consumed by the irrigation system.

Indirect cooling consists of extracting some stored heat within the PV panel due to evaporation of a residual water layer formed when irrigation ends. This stage lasts t_c minutes and may maintain or reduce the operating temperature of a PV panel with respect to the operating temperature reached when irrigation ends. The results indicate that there is a relationship between t_c and solar irradiation, as shown in Fig. 15. This layer may extend the irrigation effect by up to 1–2 min for high solar irradiation levels (>800 W/m^2) and may last 6 min or more for lower solar irradiation levels (<400 W/m^2). Such results are valid for wind speeds of 0.5–1.0 m/s. The thermal behaviour of this indirect cooling stage is similar to evaporative cooling from sprinkling, which was studied in detail by Zilli et al. (2018) and Bai et al. (2016).

The transient heating process is the third stage that a PV panel exhibits when irrigated without a continuous regimen. This

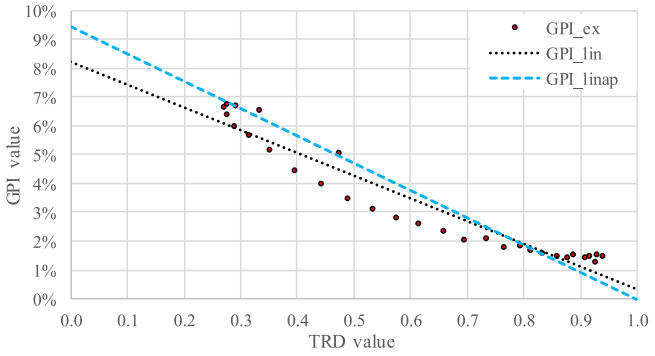

Fig. 11. Average GPI indices with respect to irrigation time and non-irrigation time.

process describes the increased operating temperature of a PV panel due to stored heat and can be characterized in terms of the *TRD* for several solar irradiation levels, as shown in Fig. 10a. This variation in stored heat is analogous to a charging capacitor, therefore is possible to estimate a value for a heating time constant τ_h. According to obtained results, τ_h is 6–7 min for high solar irradiation levels (>800 W/m^2), around 8 min for solar irradiation ranging from 600 W/m^2 to 800 W/m^2, and approximately 10 min for values less than 600 W/m^2.

The identification and characterization of the indirect cooling stage and the effect of the flow rate allows the deeper understanding of the thermal transient behaviour of the PV panel when is irrigated, which must to consider in the development of the transient models, such as the one proposed by Schiro et al. (2017).

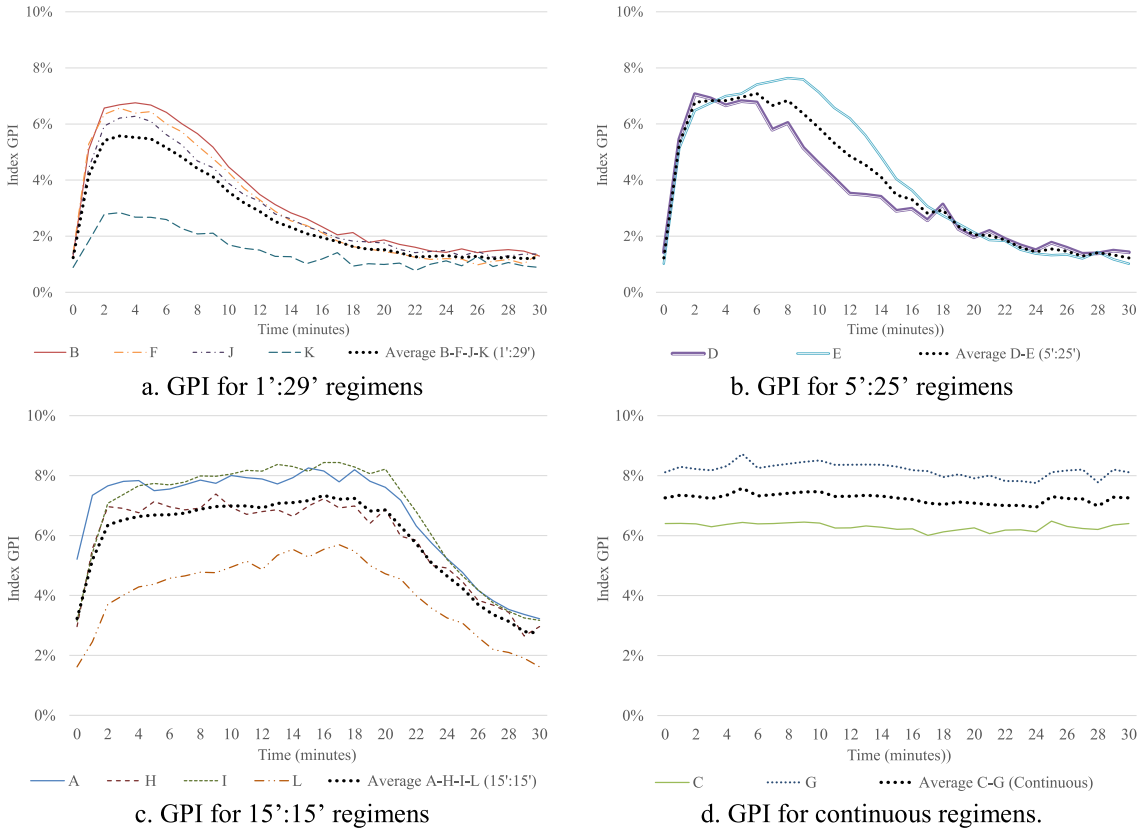

Fig. 12. Average GPI indices with respect to irrigation time and non-irrigation time.

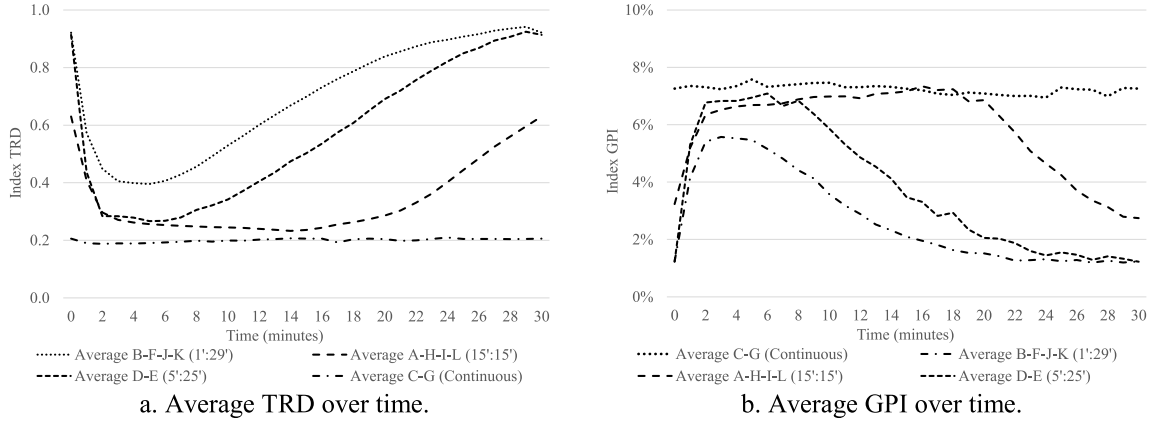

Fig. 13. TRD and GPI indices for various operation cycles.

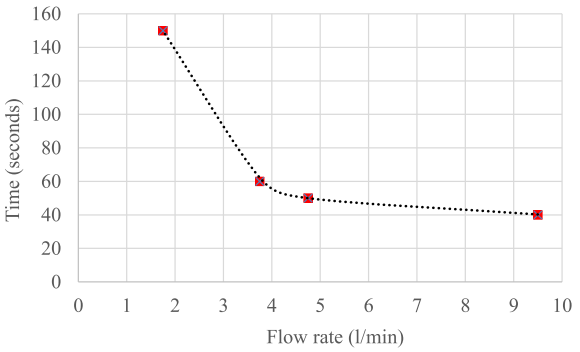

Fig. 14. Average time constant values for direct cooling (τ_{dc}) in an irrigated PV panel with respect to flow rate.

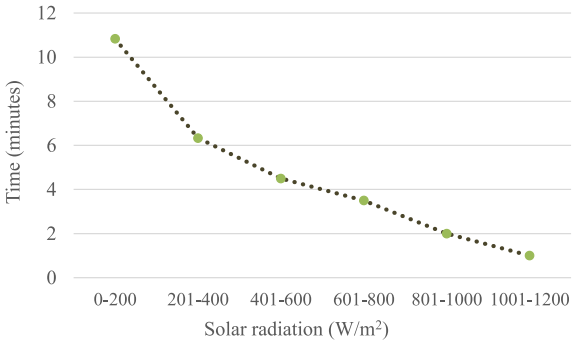

Fig. 15. Variation in the average evaporation time for a residual water layer with respect to solar irradiation.

3.5. Additional generated energy due to irrigation

In general, articles describe the effect of irrigation on power output, nevertheless there is little information regarding the feasibility of this cooling method. Therefore, information regarding the net energy benefit (*NEB*) provided by an irrigation system will facilitate economic cost–benefit studies, as proposed by Duck et al. (2018).

In this experimental setup, E_{cont} has a value of 2 Wh per day and is equivalent to a constant power consumption of 0.25 W during 8 h of service (8 a.m. to 4 p.m.). Since a controller has several outputs, it may be used to control several water pumps; therefore, $E_{is} = E_{wp} + E_{cont}/n_{PV}$ as shown in Eq. (3).

Table 5 shows E_{pw} and E_{is} values for n_{PV} equal to 1 and 10, where P_{wp} is equal to 5 W, 10 W, and 20 W for a total of 17 operation cycles per day (each 30 min over 8 h). The data show that E_{cont} can be a significant portion of E_{is}, between 20% and 58% when $n_{PV} = 1$ for irrigation times of 1 min and 5 min. Likewise, E_{cont} may be disregarded for all values of P_{wp} and t_a when $n_{PV} = 10$, as its contribution is between 0.07% and 12%. Therefore, it is advisable to use a controller for several PV panels simultaneously and it is possible to consider that $E_{is} \approx E_{wp}$ and to analyse the *NEB* as a function of P_{wp}.

Fig. 16a shows *NEB* per irrigation interval of 30 min (NEB_{30}) is equal to the energy generated by a PV panel because the energy consumed by the irrigation system is disregarded ($E_{is} = 0$). Therefore, NEB_{30} is positive for every time and every regimen; in addition, each curve in the discontinuous regimen contains two parts: a growing linear trend during irrigation and an evaporative time, and a slow increased during non-irrigation time eventually saturating at a constant value. Irrigation of PV panels may occur without energy consumption when the water is supplied directly by the building's water network. Greater values of additional accumulated energy for $t = 30$ min are produced by regimens with greater irrigation time (A, C, G, H, and I), from which is possible to an obtain average $NEB_{30} = 5.2$ Wh; while regimen K registers the worst performance ($NEB_{30} \approx 0.5$ Wh) due to the low irrigation time (1′) and low flow rate (1.75 l/min).

When $P_{wp} > 0$ W, each NEB_{30} curve in the discontinuous regimen contains two parts. First, the net energy decreases linearly during irrigation due the power consumption being greater than the additional generated power. This is followed by a slow increase during non-irrigation time that may or may not compensate the energy consumption and produce an energy benefit from irrigation. Fig. 16b shows NEB_{30} curves for $P_{wp} = 20$ W.

Fig. 17 shows the daily accumulated net energy as a function of P_{wp}. These value are referenced to a 255 W PV panel, which generates 1.0 kWh per day on average from solar irradiation in Bucaramanga city. The maximum increase is 100 Wh at $P_{wp} = 0$, which is equivalent to 10% for continuous regimens and 15′:15′ regimens. Likewise, the maximum loss is 170 Wh at $P_{wp} = 25W$, which is equivalent to 17% in the continuous regimens (C and G). All curves exhibit a negative slope caused by power consumption in the irrigation system. These curves are steeper for longer irrigation times and greater P_{si} values.

Results indicate that regimens with irrigation times of 1 min (B, F, J, and K) and 5 min (D and E) may produce energy benefits for every P_{wp} value. Continuous regimens cause unfeasible irrigation situations if $P_{wp} \geq 7$ W. In this case, the better options are

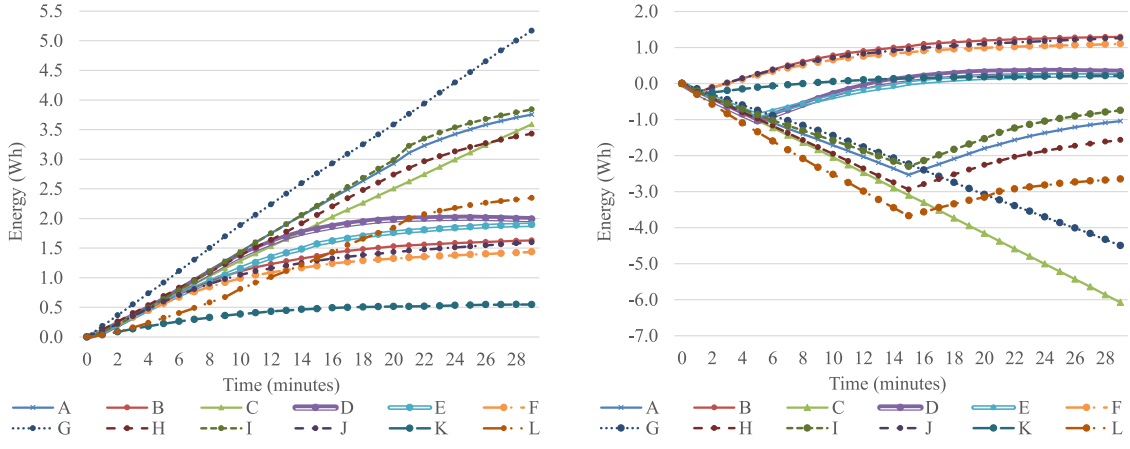

a. Case $P_{wp} = 0\ W$ b. Case $P_{wp} = 20\ W$

Fig. 16. Average accumulated additional net energy in a 30 min time window.

Table 5
Estimation of the daily energy consumption by the water pump (E_{wp}) and irrigation system per PV panel (E_{is}) considering the operation of a controller (E_{cont}) for $n_{PV} = 1$, $n_{PV} = 10$, and several values of P_{wp}.

P_{wp} (W)	E_{wp} (Wh)				E_{is} (Wh) for $n_{PV} = 1$				E_{is} (Wh) for $n_{PV} = 10$			
	t_a (minutes)				t_a (minutes)				t_a (minutes)			
	1	5	15	30	1	5	15	30	1	5	15	30
5	1.42	2.01	8.53	72.50	3.42	4.01	10.53	74.50	1.62	2.21	8.73	72.70
10	2.83	4.01	17.06	145.00	4.83	6.01	19.06	147.00	3.03	4.21	17.26	145.20
20	5.67	8.03	34.12	290.00	7.67	10.03	36.12	292.00	5.87	8.23	34.32	290.20

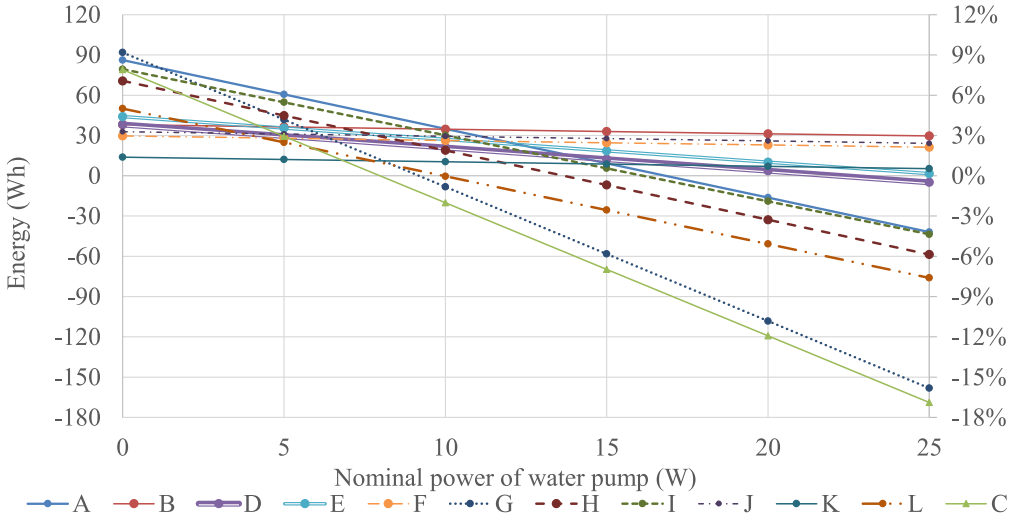

Fig. 17. Daily generated additional energy for each regimen with respect to P_{wp}.

regimens B, F, and J, which have irrigation times of 1 min and flow rates equal to or greater than 3.75 l/min. The best option is regimen J because its low flow rate allows one to select a water pump that consumes less power, which favours the energetic and financial feasibility of the irrigation system. Fig. 18 shows these results more clearly, although these curves for regimens with flow rates of 1.75 l/min (L and K) are excluded due to their reduced energy contribution. Specifically, the daily additional energy results from continuous irrigation are comparable when one considers the findings reported by Smith et al. (2014), Odeh and Behnia (2009), and Tomar et al. (2018).

With based on from the cut-off points for the daily additional energy curves and the horizontal axis (0 Wh) in Figs. 17 and 18, it is possible to estimate the maximum power consumption of the water pump (P_{wp_max}) for each type of regimen. P_{wp_max} is approximately 8–10 W, 10–16 W, 24–26 W, and 90–110 W and for the continuous irrigation regimens (C and G), 15′:15′ regimens (A, H, I, and L), 5′:25′ regimens (D and E), and 1′:29′ regimens, respectively; this value is approximately 3 W for regimen K due to the modest profit.

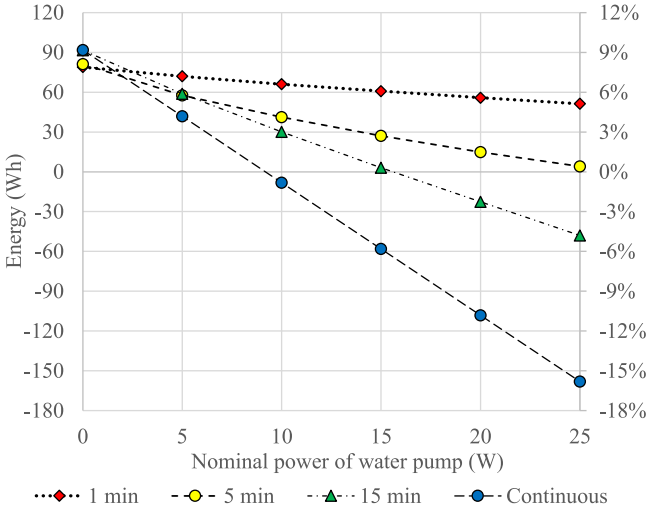

Fig. 18. Daily additional energy generated for each irrigation time with respect to P_{wp}.

4. Conclusions

Continuous and discontinuous irrigation regimens for PV panels were experimentally studied to investigate the effects of irrigation time and flow rate on the operating temperature and output power in order to better understand the benefits provided by this cooling method.

The characterization of the irrigation regimens consisted mainly of analysing the transient cooling and heating processes for a PV panel using the *TRD* and *GPI* indices, quantifying the additional generated energy, and estimating the net energy benefit while considering the energy consumed by the irrigation system.

A PV panel exhibits transient cooling and heating processes when irrigated with a discontinuous regimen during an operation cycle (t_a: t_b). Cooling occurs in two stages, direct cooling and indirect cooling. Direct cooling occurs while a water film runs over the front surface of the PV panel and extracts stored heat. Indirect cooling consists of heat extraction of stored heat within the PV panel due to evaporation of a residual water layer formed when irrigation ends. The transient heating process is the third stage and describes the increasing operating temperature of a PV panel due stored heat.

The average curves of the *TRD* index show that cooling and heating transients exhibit similar normalized behaviour for solar irradiation values greater than 200 W/m^2, while these transients are slow and produce a reduced energy benefit for solar irradiation values lower than 200 W/m^2. For that reason, the operation of the irrigation system can be dismissed in this range due to the low energy contribution.

An analysis of the discontinuous irrigation regimens indicates that an irrigation time of 1 min and a flow rate of 3.75 l/min can extract approximately 70% of the overheating that a PV panel exhibits with respect to ambient temperature. Likewise, it was also determined that a flow rate of 3.75 l/min (2.34 l/min/m^2) produces practically the same benefit as a greater flow rate, e.g., 4.75 l/min (2.97 l/min/m^2) or 9.5 l/min (5.94 l/min/m^2). The transient cooling produced by this flow rate was found to have a time constant of 60 s. This flow rate value is fundamental for selecting a water pump with the lowest power consumption, which is the primary factor determining the feasibility of the irrigation system for PV panels.

The increased output power due to irrigation depends on the value of solar irradiation, where the average increase is 0.5%–2.0% for 400 W/m^2 or lower, 2%–5% for values between 400 W/m^2 and 800 W/m^2, and 5%–10% for 800 W/m^2 or greater. This increase can reach up to 20% when solar irradiation is high (>800 W/m^2).

The maximum energy increase achieved by irrigation is 10% of the daily accumulated net energy for continuous regimens and the 15′:15′ regimens for a submergible pump power, P_{wp}, of 0 W. All regimens register a positive value for $P_{wp} = 0$. However, the curves have a negative slope caused by power consumption in the irrigation system as P_{wp} increases, and these are steeper for greater values of P_{si} and longer irrigation time.

The present study represents an initial step toward better understanding the performance of cooling systems for PV panels in tropical conditions. Understanding the thermal transients of PV panels during irrigation will facilitate the design and operation of cooling systems and ensure their feasibility. Future studies should focus on determining when and how much time a PV panel should be irrigated in order to ensure that the additional energy generation compensates the energy consumed by the irrigation system and produces a surplus sufficient for ensuring the financial feasibility of the system. One option is to develop predictive models for the operating temperature of irrigated PV panels. TRD curves can also be used to estimate the effect of irrigation as a function of the flow-rate, operating irrigation regimen, and solar irradiation.

Acknowledgements

The authors wish to thank the Department of Electrical, Electronics and Telecommunications Engineering (Escuela de Ingenierías Eléctrica, Electrónica y de Telecomunicaciones) and the Vicerectorate for Research and Extension (Vicerrectoría de Investigación y Extensión) from the Universidad Industrial de Santander (Project 8585) and the Administrative Department of Science, Technology and Innovation (Departamento Administrativo de Ciencia, Tecnología e Innovación) — COLCIENCIAS, Colombia (Project – Contract FP44842-040-2017 – Funding source).

References

Alami, A.H., 2014. Effects of evaporative cooling on efficiency of photovoltaic modules. Energy Convers. Manage. 77, 668–679. http://dx.doi.org/10.1016/j.enconman.2013.10.019.

Bahaidarah, H.M., Rehman, S., Gandhidasan, P., Tanweer, B., 2013. Experimental evaluation of the performance of a photovoltaic panel with water cooling. In: Photovoltaic Specialists Conference (PVSC), 2013 IEEE 39th. Tampa, Florida, USA, pp. 2987–2991.

Bai, A., et al., 2016. Technical and economic effects of cooling of monocrystalline photovoltaic modules under hungarian conditions. Renew. Sustain. Energy Rev. 60, 1086–1099. http://dx.doi.org/10.1016/j.rser.2016.02.003.

Chemisana, D., Lamnatou, C., 2014. Photovoltaic-green roofs: An experimental evaluation of system performance. Appl. Energy 119, 246–256. http://dx.doi.org/10.1016/j.apenergy.2013.12.027.

Duck, B.C., Fell, C.J., Anderson, K.F., Sacchetta, C., Du, Y., Zhu, Y., 2018. Determining the value of cooling in photovoltaics for enhanced energy yield. Sol. Energy 159 (2017), 337–345. http://dx.doi.org/10.1016/j.solener.2017.11.004.

Ebaid, M.S.Y., Ghrair, A.M., Al-Busoul, M., 2018. Experimental investigation of cooling photovoltaic (PV) panels using (TiO2) nanofluid in water -polyethylene glycol mixture and (Al2O3) nanofluid in water- cetyltrimethylammonium bromide mixture. Energy Convers. Manage. 155 (2017), 324–343. http://dx.doi.org/10.1016/j.enconman.2017.10.074.

George, G., Kanavas, X., Zissopoulos, D., 2013. Adam, intelligent integrated self-enhanced photovoltaic panel with rainwater harvesting for irrigation, unit cooling and cleaning. In: Proceedings of the 24th International Conference on European Association for Education in Electrical and Information Engineering, EAEEIE 2013. pp. 174–177. http://dx.doi.org/10.1109/EAEEIE.2013.6576524.

Habiballahi, M., Ameri, M., Mansouri, S.H., 2015. Efficiency improvement of photovoltaic water pumping systems by means of water flow beneath photovoltaic cells surface. J. Solar Energy Eng. 137 (4), 044501. http://dx.doi.org/10.1115/1.4029932.

a Hussien, H., Numan, A.H., Abdulmunem, A.R., 2015. Improving of the photovoltaic / thermal system performance using water cooling technique. IOP Conf. Ser.: Mater. Sci. Eng. 78, 012020. http://dx.doi.org/10.1088/1757-899X/78/1/012020.

Hussien, H.A., Numan, A.H., Abdulmunem, A.R., 2015. Improving of the photovoltaic / thermal system performance using water cooling technique. IOP Conf. Ser.: Mater. Sci. Eng. 78 (3), 012020. http://dx.doi.org/10.1088/1757-899X/78/1/012020.

Ju, F., Fu, X., 2011. Research on impact of dust on solar photovoltaic(PV) performance. In: 2011 International Conference on Electrical and Control Engineering, ICECE 2011 - Proceedings. pp. 3601–3606. http://dx.doi.org/10.1109/ICECENG.2011.6058487.

Kane, A., Verma, V., Singh, B., 2017. Optimization of thermoelectric cooling technology for an active cooling of photovoltaic panel. Renew. Sustain. Energy Rev. 75 (2016), 1295–1305. http://dx.doi.org/10.1016/j.rser.2016.11.114.

Kordzadeh, A., 2010. The effects of nominal power of array and system head on the operation of photovoltaic water pumping set with array surface covered by a film of water. Renew. Energy 35 (5), 1098–1102. http://dx.doi.org/10.1016/j.renene.2009.10.024.

Krauter, S., 2004. Increased electrical yield via water flow over the front of photovoltaic panels. Sol. Energy Mater. Sol. Cells 82 (1–2), 131–137. http://dx.doi.org/10.1016/j.solmat.2004.01.011.

Meyer, E.L., Busiso, M., 2012. Comparative study of a directly cooled PV water heating system to a naturally cooled module in South Africa. In: Conference Record of the IEEE Photovoltaic Specialists Conference. pp. 1296–1299. http://dx.doi.org/10.1109/PVSC.2012.6317839.

Moharram, K.A., Abd-Elhady, M.S., Kandil, H.A., El-Sherif, H., 2013. Enhancing the performance of photovoltaic panels by water cooling. Ain Shams Eng. J. 4 (4), 869–877. http://dx.doi.org/10.1016/j.asej.2013.03.005.

Molki, A., 2011. Temperature effect on photovoltaic cells. Phys. Educ. 46 (5), 523–525. http://dx.doi.org/10.1088/0031-9120/46/5/F08.

Nagengast, A., Hendrickson, C., Scott Matthews, H., 2013. Variations in photovoltaic performance due to climate and low-slope roof choice. Energy Build. 64, 493–502. http://dx.doi.org/10.1016/j.enbuild.2013.05.009.

Nižetić, S., Giama, E., Papadopoulos, A.M., 2018. Comprehensive analysis and general economic-environmental evaluation of cooling techniques for photovoltaic panels, Part II: Active cooling techniques. Energy Convers. Manage. 155 (2017), 301–323. http://dx.doi.org/10.1016/j.enconman.2017.10.071.

Nižetić, S., Čoko, D., Yadav, A., Grubišić-Čabo, F., 2016. Water spray cooling technique applied on a photovoltaic panel: The performance response. Energy Convers. Manage. 108, 287–296. http://dx.doi.org/10.1016/j.enconman.2015.10.079.

Odeh, S., Behnia, M., 2009. Improving photovoltaic module efficiency using water cooling. Heat Transf. Eng. 30 (6), 499–505. http://dx.doi.org/10.1080/01457630802529214.

Osma-Pinto, G., Amado-Duarte, L., Villamizar, R., Ordoñez, G., 2015. Building automation systems as tool to improve the resilience from energy behavior approach. Procedia Eng. 118, 861–868. http://dx.doi.org/10.1016/j.proeng.2015.08.524.

Ramkumar, R., Kesavan, M., Raguraman, C.M., Ragupathy, A., 2016. Enhancing the performance of photovoltaic module using clay pot evaporative cooling water. In: 2016 International Conference on Energy Efficient Technologies for Sustainability (ICEETS). pp. 217–222. http://dx.doi.org/10.1109/ICEETS.2016.7582929.

Reindl, T., et al., 2012. Investigation of the performance of commercial photovoltaic modules under tropical conditions. Japan. J. Appl. Phys. 51, 4. http://dx.doi.org/10.1143/jjap.51.10nf11.

Sainthiya, H., Beniwal, N.S., Garg, N., 2018. Efficiency improvement of a photovoltaic module using front surface cooling method in summer and winter conditions. J. Solar Energy Eng. 140 (6), 061009. http://dx.doi.org/10.1115/1.4040238.

Sargunanathan, S., Elango, A., Mohideen, S.T., 2016. Performance enhancement of solar photovoltaic cells using effective cooling methods: A review. Renew. Sustain. Energy Rev. 64, 382–393. http://dx.doi.org/10.1016/j.rser.2016.06.024.

Saxena, A., Deshmukh, S., Nirali, S., Wani, S., 2018. Laboratory based experimental investigation of photovoltaic (PV) thermo-control with water and its proposed real-time implementation. Renew. Energy 115, 128–138. http://dx.doi.org/10.1016/j.renene.2017.08.029.

Schiro, F., Benato, A., Stoppato, A., Destro, N., 2017. Improving photovoltaics efficiency by water cooling: Modelling and experimental approach. Energy 137, 798–810. http://dx.doi.org/10.1016/j.energy.2017.04.164.

Siecker, J., Kusakana, K., Numbi, B.P., 2017. A review of solar photovoltaic systems cooling technologies. Renew. Sustain. Energy Rev. 79, 192–203. http://dx.doi.org/10.1016/j.rser.2017.05.053.

Smith, M.K., Wamser, C.C., James, K.E., Moody, S., Sailor, D.J., Rosenstiel, T.N., 2013. Effects of natural and manual cleaning on photovoltaic output. J. Solar Energy Eng.-Trans. ASME 135, 4. http://dx.doi.org/10.1115/1.4023927.

Smith, M.K., et al., 2014. Water cooling method to improve the performance of field-mounted, insulated, and concentrating photovoltaic modules. J. Solar Energy Eng. Trans. ASME 136, 1–4. http://dx.doi.org/10.1115/1.4026466.

Teo, H.G., Lee, P.S., a Hawlader, M.N., 2012. An active cooling system for photovoltaic modules. Appl. Energy 90 (1), 309–315. http://dx.doi.org/10.1016/j.apenergy.2011.01.017.

Tomar, V., Tiwari, G.N., Bhatti, T.S., Norton, B., 2018. Thermal modeling and experimental evaluation of five different photovoltaic modules integrated on prototype test cells with and without water flow. Energy Convers. Manage. 165, 219–235. http://dx.doi.org/10.1016/j.enconman.2018.03.039.

Vergara-Barrios, P.P., Rey-López, J.M., Osma-Pinto, G.A., Ordóñez Plata, G., 2014. Evaluación del potencial solar y eólico del campus central de la Universidad Industrial de Santander y la ciudad de Bucaramanga, Colombia. Rev. UIS Ing. 13 (2), 49–57.

Wang, J.C., et al., 2018. On enhancing energy harvesting performance of the photovoltaic modules using an automatic cooling system and assessing its economic benefits of mitigating greenhouse effects on the environment. J. Power Sources 376 (1), 55–65. http://dx.doi.org/10.1016/j.jpowsour.2017.11.051.

Zilli, B.M., et al., 2018. Performance and effect of water-cooling on a microgeneration system of photovoltaic solar energy in Paraná Brazil. J. Cleaner Prod. 192, 477–485. http://dx.doi.org/10.1016/j.jclepro.2018.04.241.